


Article

Fabrication of Manganese Oxide/PTFE Hollow Fiber Membrane and Its Catalytic Degradation of Phenol

Yan Wang¹, Diefei Hu¹, Zhaoxia Zhang², Juming Yao^{2,3}, Jiri Militky⁴ , Jakub Wiener⁴, Guocheng Zhu^{1,*} and Guoqing Zhang^{2,*}

¹ College of Textile Science and Engineering, Zhejiang Sci-Tech University, Hangzhou 310018, China; amywang1021@hotmail.com (Y.W.); hudiefei1027@163.com (D.H.)

² School of Materials Science and Engineering, Zhejiang Sci-Tech University, Hangzhou 310018, China; zhangzx@zstu.edu.cn (Z.Z.); yaoj@zstu.edu.cn (J.Y.)

³ School of Materials Science and Chemical Engineering, Ningbo University, Ningbo 315201, China

⁴ Faculty of Textile Engineering, Technical University of Liberec, 46117 Liberec, Czech Republic; jiri.militky@tul.cz (J.M.); jakub.wiener@tul.cz (J.W.)

* Correspondence: gchengzhu@zstu.edu.cn (G.Z.); zgq@zstu.edu.cn (G.Z.)

Abstract: P-aminophenol is a hazardous environmental pollutant that can remain in water in the natural environment for long periods due to its resistance to microbiological degradation. In order to decompose p-aminophenol in water, manganese oxide/polytetrafluoroethylene (PTFE) hollow fiber membranes were prepared. MnO₂ and Mn₃O₄ were synthesized and stored in PTFE hollow fiber membranes by injecting MnSO₄·H₂O, KMnO₄, NaOH, and H₂O₂ solutions into the pores of the PTFE hollow fiber membrane. The resultant MnO₂/PTFE and Mn₃O₄/PTFE hollow fiber membranes were characterized using scanning electron microscopy (SEM), X-ray photoelectron spectroscopy (XPS), and thermal analysis (TG). The phenol catalytic degradation performance of the hollow fiber membranes was evaluated under various conditions, including flux, oxidant content, and pH. The results showed that a weak acid environment and a decrease in flux were beneficial to the catalytic degradation performance of manganese oxide/PTFE hollow fiber membranes. The catalytic degradation efficiencies of the MnO₂/PTFE and Mn₃O₄/PTFE hollow fiber membranes were 70% and 37% when a certain concentration of potassium monopersulfate (PMS) was added, and the catalytic degradation efficiencies of MnO₂/PTFE and Mn₃O₄/PTFE hollow fiber membranes were 50% and 35% when a certain concentration of H₂O₂ was added. Therefore, the manganese oxide/PTFE hollow fiber membranes represent a good solution for the decomposition of p-aminophenol.



Citation: Wang, Y.; Hu, D.; Zhang, Z.; Yao, J.; Militky, J.; Wiener, J.; Zhu, G.; Zhang, G. Fabrication of Manganese Oxide/PTFE Hollow Fiber Membrane and Its Catalytic Degradation of Phenol. *Materials* **2021**, *14*, 3651. <https://doi.org/10.3390/ma14133651>

Academic Editor: Bojana Vončina

Received: 20 May 2021

Accepted: 24 June 2021

Published: 30 June 2021

Publisher's Note: MDPI stays neutral with regard to jurisdictional claims in published maps and institutional affiliations.



Copyright: © 2021 by the authors. Licensee MDPI, Basel, Switzerland. This article is an open access article distributed under the terms and conditions of the Creative Commons Attribution (CC BY) license (<https://creativecommons.org/licenses/by/4.0/>).

Keywords: manganese oxide; PTFE hollow fiber membrane; catalyst; degradation; phenol

1. Introduction

Organic wastewater treatment is an important issue owing to its impact on the environment and human health. P-aminophenol, a well-known hazardous environmental pollutant, can remain in water in the natural environment for long periods due to its resistance to microbiological degradation [1,2]. Various symptoms, including skin, eye, and respiratory system irritation, and detrimental effects in the blood and kidneys, were described as a result of p-aminophenol exposure [3].

Conventional methods, such as coagulation, microbial degradation, absorption in activated carbon, incineration, biosorption, filtration, and sedimentation, have been used to treat various kinds of organic wastewater [4–6]. Many forms of membrane filter technology, including ultrafiltration, nanofiltration, and reverse osmosis, are commonly used to separate and enrich organic matter from the wastewater, after which the obtained wastes need to be further decomposed into unarmful smaller molecules [7–9].

In recent years, a promising approach known as the advanced oxidation process (AOP) was developed to dispose dye wastewater [10]. AOP generally utilizes strong oxidizing

species, such as -OH radicals, to trigger a sequence of degradation reactions and break down the dye macromolecule into smaller and unarmful substances [11]. In wastewater treatment, AOPs usually refer to specific subsets of processes that involve O_3 , H_2O_2 , and/or ultraviolet (UV) light. However, AOPs can also be used to refer to a more general group of processes that involve photocatalytic oxidation, ultrasonic cavitation, electron-beam irradiation, and Fenton's reaction [12].

In the majority of AOPs, a catalyst is necessary to promote oxidizing species generation. Several metal oxides, such as titanium dioxide (TiO_2), zinc oxide (ZnO), cerium dioxide (CeO_2), have been demonstrated to be good catalysts [13–16]. However, most of the reported catalysis reactions were carried out in homogeneous media, which involves mixing catalysis particles with wastewater, and results in a mixture that is difficult to recycle.

In order to overcome the disadvantages of the aforementioned methods, fixing the catalytic agent onto a suitable supporting material is a feasible strategy. Organic polymer, zeolites, cellulose fibers, and silica have been reported as suitable supporting materials [16–18]. However, there are still several concerns regarding the loading of catalysts onto carriers. Firstly, the catalyst must attach to the carrier tightly and cannot be removed easily, which limits the use of certain highly efficient catalysts, such as TiO_2 and ZnO . Secondly, it is difficult to encourage the dye molecules in the wastewater to come into contact with catalyst particles, which has a negative effect on catalytic efficiency.

Poly(tetrafluoroethylene) (PTFE) membranes are widely used for water purification [9,19] due to their outstanding chemical stability, high heat resistance, strong hydrophobicity, and fracture toughness [20,21]. The outstanding properties of PTFE are due to the strong C–C and C–F bonds and the carbon backbone, which is protected by a uniform helical sheath formed by the electron cloud of the fluorine atoms [22,23]. Various researchers reported that $\text{MnO}_2/\text{CeO}_2$ and MnO_2 exhibit high activity for the complete oxidation of phenol to carbon dioxide and water [24–26].

Therefore, in this work, a PTFE hollow fiber membrane (HFM) is proposed as a carrier. Moreover, manganese oxide was selected as the catalyst, which was synthesized in situ in the pores of the PTFE hollow fiber membrane to decompose the p-aminophenol in a consecutive catalytic reaction process.

2. Materials and Methods

2.1. Materials

$\text{MnSO}_4 \cdot \text{H}_2\text{O}$, NaOH , KMnO_4 , and 30% H_2O_2 at analytical reagent grade were provided by Hangzhou Huipu Chemical Instrument Co., Ltd. (Hangzhou, China), deionized water was purchased from Millipore, p-aminophenol was obtained from Hangzhou Gaojing Chemical Plant, (Hangzhou, China), and PTFE hollow fiber membrane was purchased from Motech Co., Ltd. (Tianjin, China).

2.2. Preparations of Manganese Oxide/PTFE Hollow Fiber Membrane

The conditions of the manganese oxide/PTFE hollow fiber membrane preparation were optimized by adjusting the concentration of $\text{MnSO}_4 \cdot \text{H}_2\text{O}$, the reaction time, and the temperature. The specific procedures and parameters of the preparation of the MnO_2/PTFE and $\text{Mn}_3\text{O}_4/\text{PTFE}$ hollow fiber membranes are described below.

2.2.1. MnO_2/PTFE Hollow Fiber Membrane

The $\text{MnSO}_4 \cdot \text{H}_2\text{O}$ solution at a concentration of 0.4 mol/L and KMnO_4 solution at a concentration of 0.1 mol/L were prepared in a digital control ultrasonic cleaner (model: KQ-100DB, supplier: Kunshan ultrasonic instruments Co., LTD, Kunshan, China) at a power of 100 W, a frequency of 40 KHz, and a temperature of 25 °C for 10 min. The $\text{MnSO}_4 \cdot \text{H}_2\text{O}$ solution was injected into the PTFE hollow fiber membrane using a syringe, and then the PTFE hollow fiber membrane was dried at a temperature of 75 °C for 12 h. After cooling to room temperature, the KMnO_4 solution was injected into the PTFE hollow fiber membrane using a syringe, and then the hollow fiber membrane was treated by

ultrasonic vibration at a power of 100 W, a frequency of 40 KHz, and a temperature of 25 °C for 1 h. This was done so that the KMnO_4 solution could enter into the micropores of the hollow fiber membrane, and come into adequate contact and produce a complete reaction with MnSO_4 . Thereafter, the PTFE hollow fiber membrane was dried at a temperature of 75 °C for 24 h. Finally, the MnO_2 /PTFE hollow fiber membrane was obtained. The residual MnO_2 particles in the hollow fiber were washed away using deionized water at a flow rate of 500 mL/h provided by a peristaltic pump, which is shown in Figure 1.

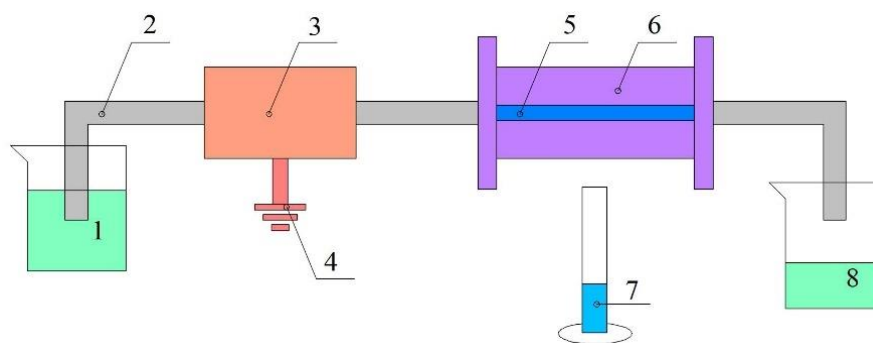
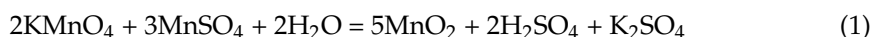


Figure 1. The setup diagram of the manganese oxide/PTFE HFM degradation: (1) p-aminophenol solution or deionized water; (2) silicone tube; (3) peristaltic pump; (4) power supply; (5) MnO_2 /PTFE or Mn_3O_4 /PTFE HFM; (6) supporter; (7) osmotic solution; (8) p-aminophenol solution or deionized water.

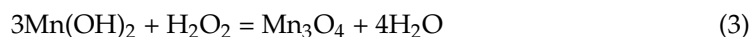
The reaction mechanism for the synthesis of MnO_2 is shown as follows:



2.2.2. Mn_3O_4 /PTFE Hollow Fiber Membrane

$\text{MnSO}_4 \cdot \text{H}_2\text{O}$ solution at a concentration of 0.5 mol/L and NaOH solution at a concentration of 0.05 mol/L were prepared in a digital control ultrasonic cleaner at a power of 100 W, a frequency of 40 KHz, and a temperature of 25 °C for 10 min. The $\text{MnSO}_4 \cdot \text{H}_2\text{O}$ solution was injected into the PTFE hollow fiber membrane using a syringe, and then the PTFE hollow fiber membrane was dried at a temperature of 75 °C for 12 h. After cooling to room temperature, the NaOH solution was injected into the PTFE hollow fiber membrane using a syringe, and then the PTFE hollow fiber membrane was dried at a temperature of 75 °C for 2 h. After cooling to room temperature, the 30% H_2O_2 was injected into the PTFE hollow fiber membrane. The resultant PTFE hollow fiber membrane was placed at a temperature of 75 °C for 24 h. Finally, the Mn_3O_4 /PTFE hollow fiber membrane was obtained. The residual Mn_3O_4 particles in the hollow fiber were washed away using the setup shown in Figure 1.

The reaction mechanism for the synthesis of Mn_3O_4 is shown as follows:



2.3. Characterization

The cross-section and inner surfaces of the hollow fiber were characterized using field-emission scanning electron microscopy (FE-SEM, Hitachi S-4800, Tokyo, Japan) at 5Kv, and the FE-SEM was equipped with energy dispersive spectroscope (EDS, Oxford instruments, Oxford, UK). The hollow fiber membrane was firstly fractured in liquid nitrogen and then coated with gold using an EMITECH SC7620 sputter coater (Quorum, East Sussex, UK) before SEM testing. The energy dispersive spectrometer (EDS) spectrum (Oxford instruments, Oxford, UK) was recorded simultaneously. The content and distribution of elements were analyzed by EDS and mapping.

The elements, chemical state, and relative content of elements on the sample surface were determined using XPS (Mode: K-Alpha, Company: Thermo Fisher Scientific, Waltham, MA, USA). Before testing, the manganese oxide/PTFE hollow fiber membranes were cleaned with deionized water.

The thermal degradation processes for PTFE and manganese oxide/PTFE hollow fiber membranes were recorded on a thermogravimetry analyzer (Mode: Pyris 1, Company: Perkinelmer, Waltham, MA, USA) at temperatures from 20–800 °C at a heating rate of 10 °C/min under a 20 mL/min N₂ gas purge. The temperature of the TGA was periodically calibrated using Al and Fe standards in the range 30–800 °C with an accuracy of ±0.1 °C.

The flux measurement was performed as follows: The flow rate was adjusted using a peristaltic pump to pass the solution through the hollow fiber membrane. The solution exuded out from the membrane wall to obtain the osmotic solution, and the flux was calculated from the mass of the osmotic solution, the surface area of the hollow fiber membrane, and the time.

The catalytic degradation test was performed as follows: The catalytic performance was estimated using UV spectrum analysis. Concentrations of neutral organic solutes in the feed and permeate solutions were measured using a UV spectrograph. The flux of the hollow fiber membranes was also measured under different operating pressures.

3. Results and Discussions

3.1. Morphology of PTFE Hollow Fiber Membrane

The cross-section and inner surface of the PTFE hollow fiber membrane are shown in Figure 2. As can be seen, it is characterized by a multilevel and regular porous structure. The wall thickness of the hollow fiber was about 250 μm. The outer layer is characterized by scarce pores and a large pore diameter of about 5–10 μm; the inner layer was smooth and contained dense pores and a small pore diameter of about 1 μm.

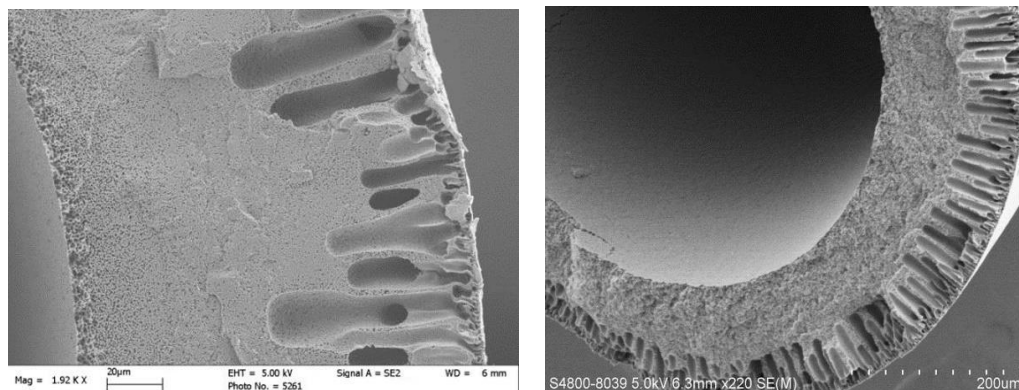


Figure 2. Cross-section and inner surface of the PTFE hollow fiber.

3.2. Mapping Image of PTFE Hollow Fiber Membrane

The distribution of manganese oxides in the membrane pores was observed using element distribution analysis. The distribution of C, F, O, and Mn in the cross-section of the manganese oxide/PTFE hollow fiber membrane was obtained using mapping.

As shown in Figure 3, manganese oxide synthesized from MnSO₄·H₂O and KMnO₄ was evenly distributed in the membrane pores. During the preparation of the manganese oxide/PTFE hollow fiber membrane, KMnO₄ permeated from the inside to the outside, resulting in a higher manganese content in the pores on the inner layer of the membrane.

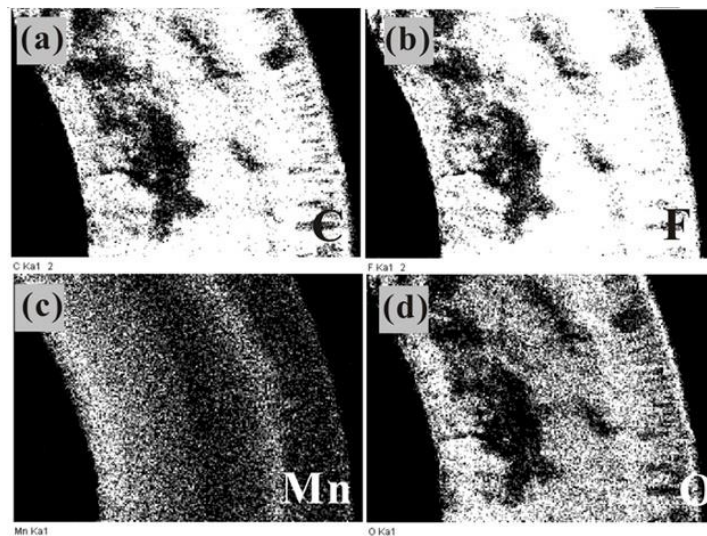


Figure 3. Mapping image of the MnO_2/PTFE HFM of: (a) C element; (b) F element; (c) Mn element; (d) O element.

As shown in Figure 4, manganese oxide synthesized from $\text{MnSO}_4 \cdot \text{H}_2\text{O}$, NaOH, and H_2O_2 was sparse and stratified in the hollow fiber, and was mainly distributed in the inner and outer layers of the cross-section; the oxygen element was uniform and compact. In the preparation process, the injected H_2O_2 permeated from the inside to the outside, so the concentration of H_2O_2 in the inner layer was higher, which made it easier to synthesize manganese oxide. Moreover, as a result of the large pore size of the outer membrane, a large amount of oxygen can be stored, which was conducive to the synthesis of manganese oxide.

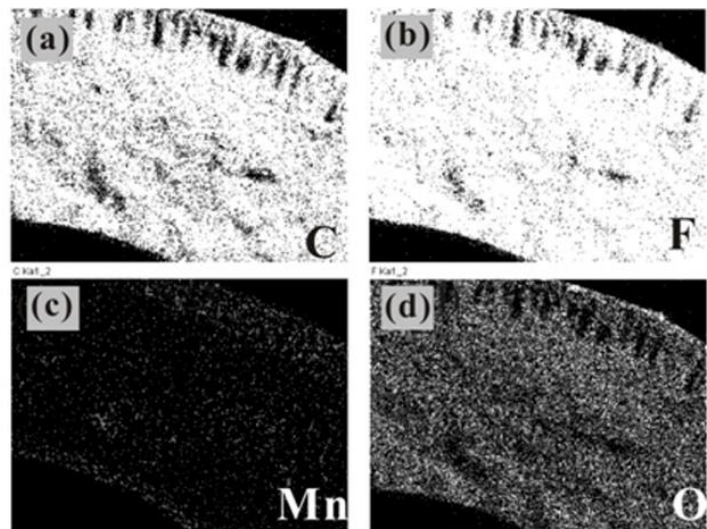


Figure 4. Mapping image of the $\text{Mn}_3\text{O}_4/\text{PTFE}$ HFM of: (a) C element; (b) F element; (c) Mn element; (d) O element.

The results also demonstrate that the content of manganese oxide synthesized in the hollow fiber membrane in the former (Figure 3) was higher than that in the latter (Figure 4).

3.3. Electronic Diffraction Spectrum

KMnO_4 , $\text{MnSO}_4 \cdot \text{H}_2\text{O}$ and $\text{MnSO}_4 \cdot \text{H}_2\text{O}$, NaOH, and H_2O_2 were used to synthesize manganese oxide in the PTFE hollow fiber membranes. The element content in the hollow fiber membrane was analyzed using electronic diffraction spectrum (EDS).

According to the EDS spectrum shown in Figure 5, only C, F, Mn, and O were found in the sample, which proved that the manganese element in the mapping came from manganese oxide. The atomic content of each element in the two kinds of manganese oxide/PTFE hollow fiber membranes are shown in Table 1.

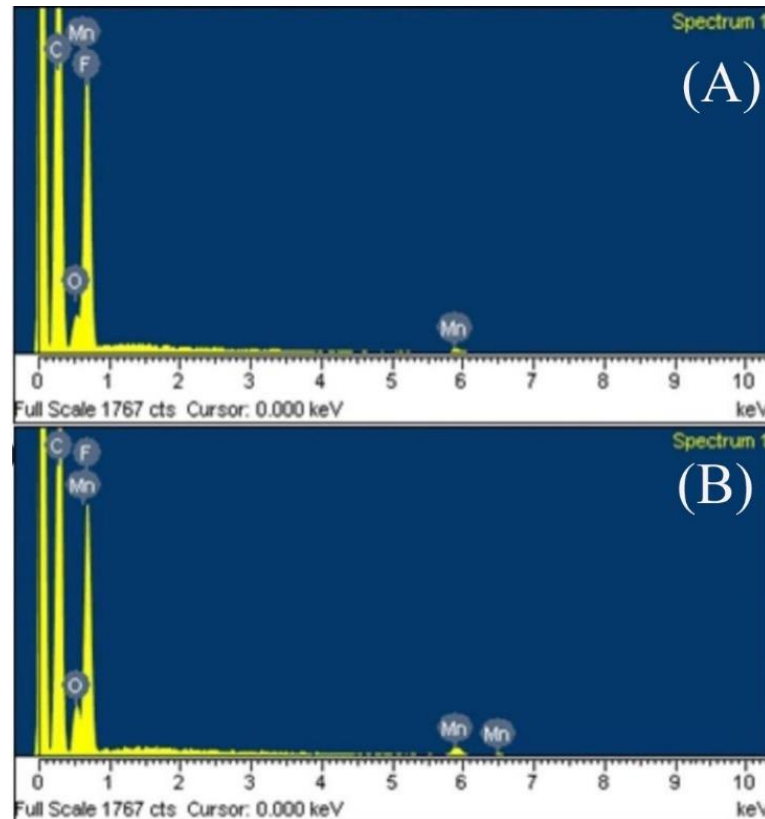


Figure 5. EDS spectrum image of: (A) MnO_2 /PTFE HFM; (B) Mn_3O_4 /PTFE HFM.

Table 1. The element contents of MnO_2 / Mn_3O_4 PTFE HFMs.

Samples	Element Content/%			
	C	F	O	Mn
PTFE HFM	68.61	31.39	/	/
MnO_2 /PTFE HFM	58.92	32.19	5.73	3.16
Mn_3O_4 /PTFE HFM	59.08	30.78	5.64	4.5

The results demonstrate that there were only C and F in the original membrane, and the atomic ratio was about 2:1 (given in Table 1), which is consistent with the atomic ratio of the molecular formula $(-\text{CF}_2-\text{CF}_2-)_n$ of PTFE. The atomic percentages of Mn and O in the MnO_2 /PTFE HFM and Mn_3O_4 /PTFE HFM were approximately 1:2 and 3:4. This reveals that the MnO_2 and Mn_3O_4 were successfully synthesized in the PTFE hollow fiber membranes.

3.4. X-ray Photoelectron Spectroscopy

In order to determine the valence state of Mn in the manganese oxide/PTFE hollow fiber membrane, the manganese oxide/PTFE hollow fiber membranes were analyzed using X-ray photoelectron spectroscopy (XPS), and the oxidation state was determined from the position of the Mn2P binding energy, as shown in Figure 6.

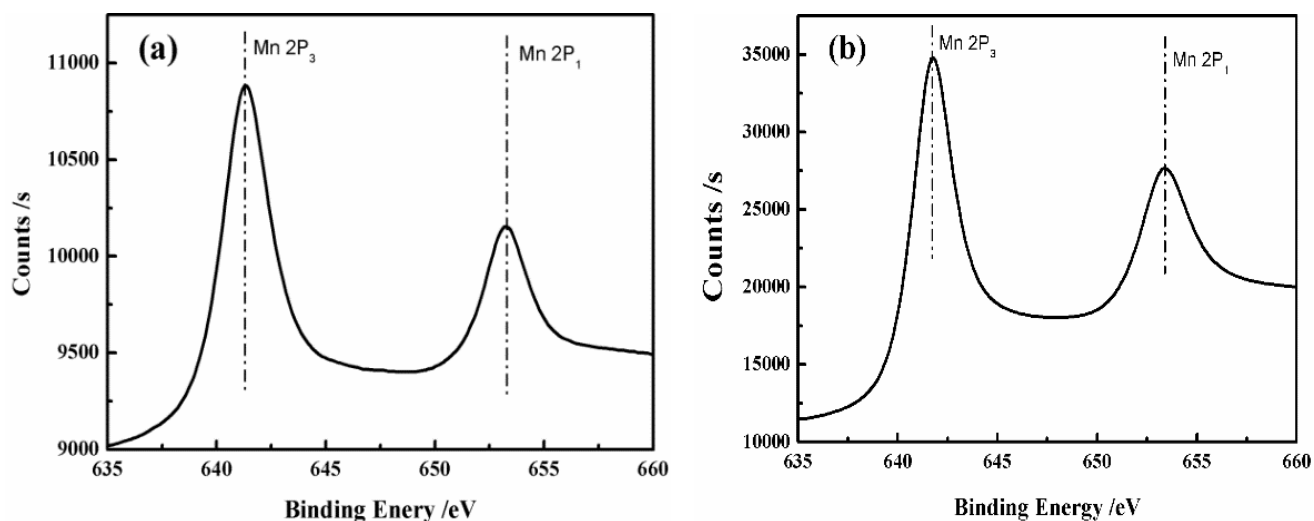


Figure 6. XPS spectra of the Mn2P region of samples: (a) Mn_3O_4 /PTFE hollow fiber membrane; (b) MnO_2 /PTFE hollow fiber membrane.

According to Kim's study [27,28], the Mn2P₃ (Mn2P₁) value of the binding energy of Mn_3O_4 was 641.01 (653.61), and the Mn2P₃ (Mn2P₁) value of the binding energy of MnO_2 was 642.61 (654.42). As shown in Table 2, the manganese oxide formed in the PTFE hollow fiber membrane by in situ synthesis was determined as Mn_3O_4 and MnO_2 , which is consistent with the experimental results from the simulated hydrothermal method.

Table 2. The binding energy of Mn 2P of MnO_2 and Mn_3O_4 .

Samples	MnO_2	Mn_3O_4
Mn 2P ₃ (eV)	642.6	641.0
Mn 2P ₁ (eV)	654.4	653.6

3.5. TG of PTFE Hollow Fiber with and without Manganese Oxide

A thermal gravimetric analysis of the PTFE, MnO_2 /PTFE, and Mn_3O_4 /PTFE hollow fiber membranes was carried out. As shown in Figure 7, when the temperature reached 600 °C, it was considered that the base film was completely burned, and the remaining residue represented the content of MnO_2 and Mn_3O_4 in the hollow fiber membrane. As shown in Table 3, more MnO_2 was loaded in the PTFE hollow fiber membrane than Mn_3O_4 .

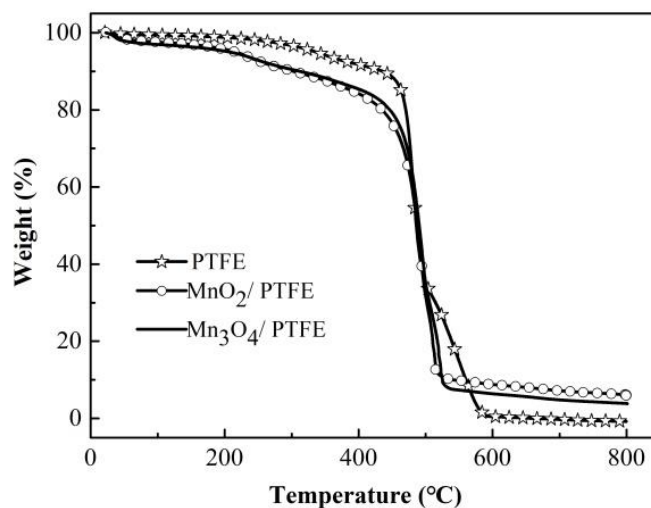


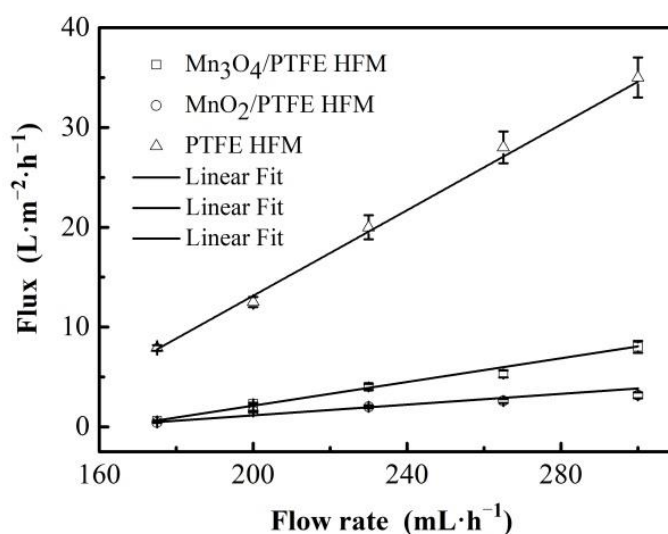
Figure 7. TG analysis of PTFE, MnO_2 /PTFE, and Mn_3O_4 /PTFE HFMs.

Table 3. Manganese oxide content in the PTFE HFMs.

Samples	MnO ₂ /PTFE HFM	Mn ₃ O ₄ /PTFE HFM	PTFE HFM
Residual content at 600 °C (%)	8.78	6.47	0.28

3.6. Flux of Membrane

The fluxes of the hollow fiber membranes are shown in Figure 8. The flux of the hollow fiber membranes increased with the increase in the inlet flow rate, and it demonstrated a linear correlation ($R^2 \geq 0.97$ for all hollow fiber membranes).

**Figure 8.** The flux of hollow fiber membranes.

On the other hand, the fluxes of the PTFE hollow fiber membranes were much higher than that of the others at 7.9, 12.5, 20, 28, and 35 L/m²/h corresponding to the flow rates of 175, 200, 230, 265, and 300 mL/h, respectively. The fluxes of the MnO₂/PTFE hollow fiber membrane were the smallest at 0.43, 1.54, 2, 2.59, and 3.16 L/m²/h at the same inlet flow rates. The flux of the Mn₃O₄/PTFE hollow fiber membrane was almost twice that of the MnO₂/PTFE hollow fiber membrane. The reason for the flux decrease could be the occupation of manganese oxide in the pores of the PTFE hollow fiber membrane. Moreover, the content of MnO₂ was about 25% higher than the content of Mn₃O₄ in the PTFE hollow fiber membrane, which can be observed in Figure 7 and Table 3.

On the contrary, the decrease in membrane flux increased the contact time between the manganese oxide and the organic matter and might improve the catalytic degradation efficiency of manganese oxide.

3.7. Effect of H₂O₂ on the Degradation of Phenol by the Manganese Oxide/PTFE Hollow Fiber Membrane

Oxidants such as hydrogen peroxide (H₂O₂) can produce hydroxyl radicals under the catalysis of catalysts. Hydroxyl radicals have a strong oxidation ability, and thus oxidize and degrade phenol.

H₂O₂ at concentrations of 0.01 mol/L, 0.02 mol/L, and 0.03 mol/L was added to the phenol solution, which was at a concentration of 50 ppm. The mixed solution was fed into the PTFE, MnO₂/PTFE, and Mn₃O₄/PTFE hollow fiber membranes through the device shown in Figure 1, and the flux was maintained at 1.5 L/m²/h. The osmotic solution was collected every 2 h, and tested using a UV spectrophotometer (Thermo Fisher Scientific, Waltham, MA, USA). The results are shown in Figure 9.

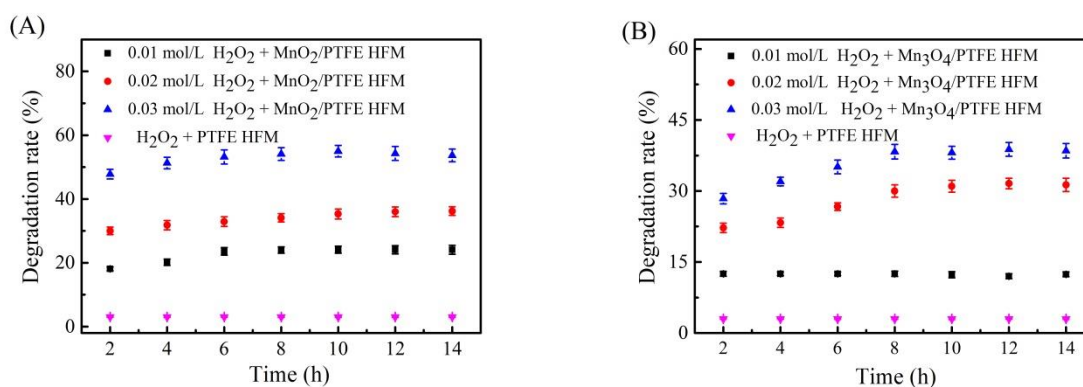


Figure 9. The influence of H₂O₂ on the degradation rate of phenol: (A) MnO₂/PTFE HFM; (B) Mn₃O₄/PTFE HFM.

It is clear to see that the degradation performance was much higher when manganese oxide was loaded in the PTFE hollow fiber membrane, and the increase in H₂O₂ concentration led to a higher degradation rate. When the H₂O₂ concentration was 0.03 mol/L, the phenol degradation efficiencies of the MnO₂/PTFE and Mn₃O₄/PTFE hollow fiber membranes were 50% and 35% after 14 h. From the mechanism, it can be inferred that the surface of MnO₂ was rich in Mn³⁺ and Mn⁴⁺ [29], while Mn₃O₄ was composed of Mn²⁺ and Mn³⁺. This ion distribution produced MnO₂ and Mn₃O₄ in the pores of the PTFE hollow fiber membrane and thus a strong catalytic reaction [30]. This catalyzed H₂O₂ to produce a large amount of substances that degrade phenol.

3.8. Effect of Peroxymonosulfate on the Degradation of Phenol by the Manganese Oxide/PTFE Hollow Fiber Membrane

According to Edy's report [31], SO₄⁻ has a higher redox potential than HO. In the presence of manganese oxide, peroxydisulfate (PMS) can form a Fenton-like system, which can produce a large amount of SO₄⁻. SO₄⁻ has strong oxidability, which has a good degradation effect on phenolic organic compounds [32,33].

PMS at concentrations of 1×10^{-4} mol/L, 3×10^{-4} mol/L, and 5×10^{-4} mol/L was added to the phenol solution, which was at a concentration of 50 ppm. The mixed solution was fed into the PTFE, MnO₂/PTFE, and Mn₃O₄/PTFE hollow fiber membranes through the device shown in Figure 1, and the flux was maintained at 1.5 L/m²/h. The osmotic solution was collected every 2 h, and tested using a UV spectrophotometer. The results are shown in Figure 10.

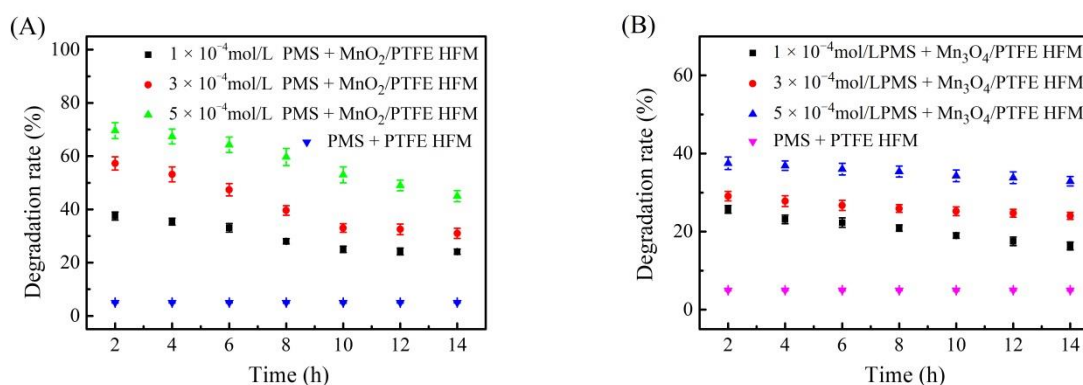


Figure 10. The influence of the concentration of PMS on the degradation of phenol: (A) MnO₂/PTFE HFM; (B) Mn₃O₄/PTFE HFM.

The degradation performance was much higher when manganese oxide was loaded in the PTFE hollow fiber membrane, and the increase in PMS concentration resulted in a higher degradation rate.

When the PMS concentration was 5×10^{-4} mol/L, the phenol degradation efficiencies of the MnO_2 /PTFE and Mn_3O_4 /PTFE hollow fiber membranes were 70% and 37% after 2 h.

It was hypothesized that the surface of MnO_2 is rich in Mn^{3+} and Mn^{4+} , and Mn_3O_4 is composed of Mn^{2+} and Mn^{3+} . This ion distribution caused the high MnO_2 and Mn_3O_4 catalytic activity in the catalytic reaction [29], and catalyzed PMS to produce a large number of substances that can effectively degrade phenol [30].

3.9. Effect of pH on the Degradation of Phenol by the Manganese Oxide/PTFE Hollow Fiber Membrane

The pH environment has a great influence on the degradation of organic matter by metal oxides [34]. In this experiment, the pH value of the phenol solution with a concentration of 50 ppm was adjusted by combining 1 mol/L sodium hydroxide and 1 mol/L hydrochloric acid. The adjusted phenol solution was fed into the MnO_2 /PTFE and Mn_3O_4 /PTFE hollow fiber membranes through the device shown in Figure 1, and the flux was maintained at $1.5 \text{ L/m}^2/\text{h}$.

It was found that in the weak acid environment, the degradation of phenol by the two kinds of the manganese oxide/PTFE hollow fiber membrane was higher (as shown in Figure 11). This may be related to the strong capacity of oxygen storage of manganese oxide. Manganese oxide catalyzes oxygen to produce oxygen anion [34–36], while H^+ promotes the degradation of organic matter. In the weak alkali environment, the decrease in phenol was relatively stable. This was hypothesized to be due to the weak acidity of phenol, which can partly react with sodium hydroxide.

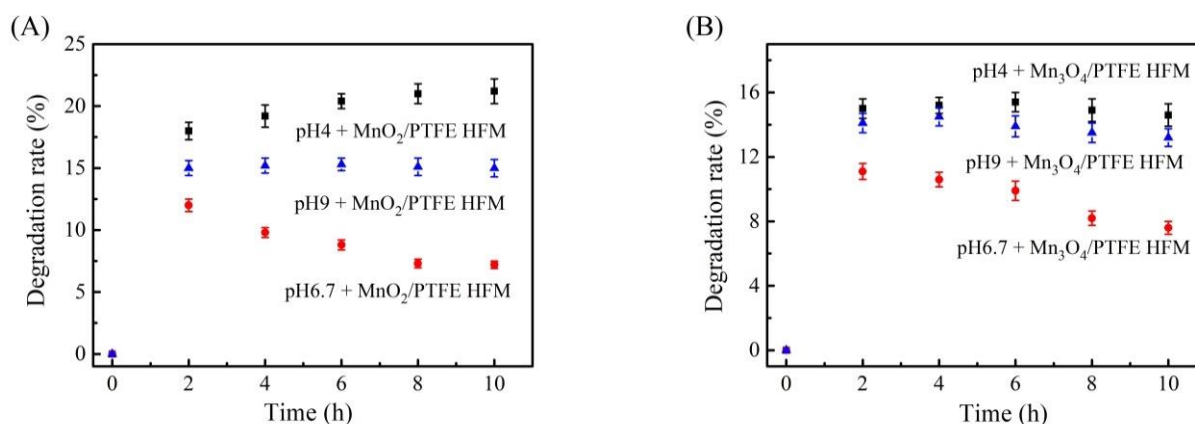


Figure 11. The influence of pH on the degradation of phenol: (A) MnO_2 /PTFE HFM (B) Mn_3O_4 /PTFE HFM.

3.10. Effect of Membrane Flux on the Degradation of Phenol by the Manganese Oxide/PTFE Hollow Fiber Membrane

Membrane flux is not only an important index for characterizing the treatment efficiency of a filtration membrane, but it also affects the catalytic degradation ability of the hollow fiber membrane. According to the following thermodynamic equation: $\Delta G = \Delta H - \Delta(S \cdot T)$, the chemical reaction takes a certain amount of time.

The flux of the solution passing through the manganese oxide/PTFE hollow fiber membrane was controlled by the peristaltic pump (as shown in Figure 1). In order to investigate the effect of membrane flux on the phenol degradation efficiencies of the manganese oxide/PTFE hollow fiber membrane, fluxes of $0.5 \text{ L/m}^2/\text{h}$, $1.5 \text{ L/m}^2/\text{h}$, and $3 \text{ L/m}^2/\text{h}$ were selected and provided by the peristaltic pump. The phenol solution at a concentration of 50 ppm containing 5×10^{-4} mol/L PMS was selected as the inlet solution.

When the membrane flux was $0.5 \text{ L/m}^2/\text{h}$, the phenol degradation rate of the MnO_2 /PTFE and Mn_3O_4 /PTFE hollow fiber membranes reached 90% and 80%, respectively. When the flux was $1.5 \text{ L/m}^2/\text{h}$, the membrane still demonstrated obvious phenol removal in a short time, but with the increase in time, the phenol degradation effect decreased. However, when the flux was $3 \text{ L/m}^2/\text{h}$, the removal efficiency of phenol was

not obvious (as shown in Figure 12). This reveals that it would take a certain reaction time for manganese oxide to catalyze PMS to produce free radicals. The smaller the flux, the more the free radicals that were produced by the manganese oxide to catalyze PMS. A longer reaction time between the organic matter and free radicals would produce an improved reaction.

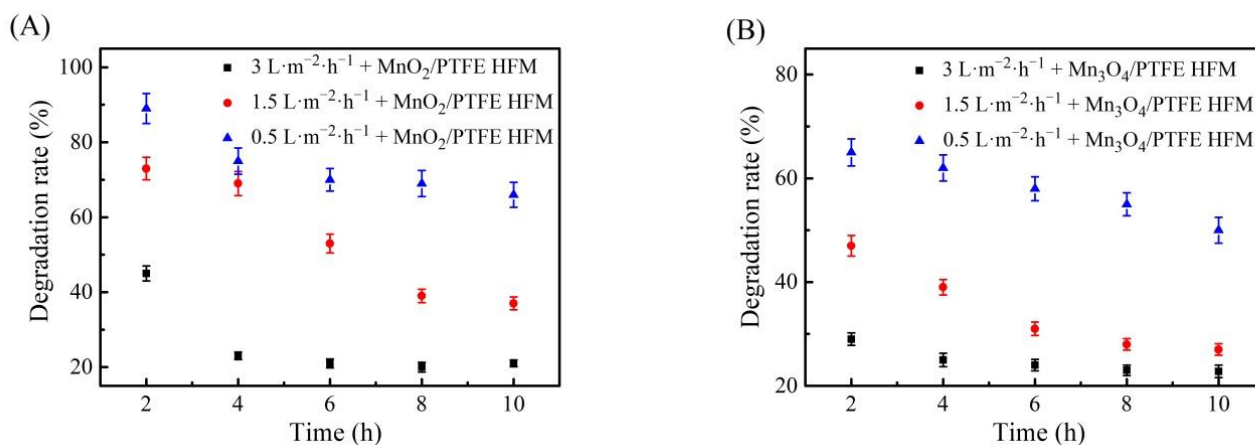


Figure 12. The influence of flux on the degradation of phenol: (A) used MnO₂/PTFE HFM; (B) Mn₃O₄/PTFE HFM.

4. Conclusions

In this paper, Mn₃O₄/PTFE and MnO₂/PTFE hollow fiber membranes were successfully prepared by in situ synthesis using two different solution systems under mild conditions and without any surfactants or additives. The flux of the manganese oxide/PTFE hollow fiber membranes decreased as compared with the PTFE hollow fiber membranes; however, their catalytic degradation of phenol improved dramatically. The phenol degradation efficiencies of the MnO₂/PTFE and Mn₃O₄/PTFE hollow fiber membranes were 50% and 35% under the 0.03 mol/L H₂O₂ condition, and were 70% and 37% under the 5×10^{-4} mol/L PMS condition. In summary, higher H₂O₂ concentrations, higher PMS concentrations, weaker acid environments, and smaller fluxes were beneficial for the catalytic degradation of phenol by the manganese oxide/PTFE hollow fiber membrane. Furthermore, this method was demonstrated to be an effective and economic way to decompose p-aminophenol.

Author Contributions: Conceptualization, G.Z. (Guoqing Zhang) and G.Z. (Guocheng Zhu); methodology, J.Y. and J.M.; validation, Y.W. and D.H.; formal analysis, Z.Z. and J.W.; investigation, Y.W. and D.H.; resources, G.Z. (Guoqing Zhang); data curation, Y.W. and D.H.; writing—original draft preparation, Y.W.; writing—review and editing, G.Z. (Guocheng Zhu); visualization, J.M. and J.W.; supervision, G.Z. (Guoqing Zhang) and G.Z. (Guocheng Zhu); project administration, G.Z. (Guoqing Zhang); funding acquisition, G.Z. (Guoqing Zhang). All authors have read and agreed to the published version of the manuscript.

Funding: This research received no external funding.

Institutional Review Board Statement: Not applicable.

Informed Consent Statement: Not applicable.

Data Availability Statement: Data available in a publicly accessible repository.

Acknowledgments: The work was supported by the National Natural Science Foundation of China (Grant No. 22075252) and by the Scientific Research Foundation of Zhejiang Sci-Tech University (Grant No.: 18012214-Y, 16012168-Y).

Conflicts of Interest: The authors declare no conflict of interest.

References

1. Khan, S.A.; Hamayun, M.; Ahmed, S. Degradation of 4-aminophenol by newly isolated *Pseudomonas* sp. strain ST-4. *Enzym. Microb. Technol.* **2006**, *38*, 10–13. [[CrossRef](#)]
2. Hong, X.; Duan, C.F.; Zhang, Z.F.; Chen, J.Y.; Lai, C.Z.; Lian, M.; Liu, L.J.; Hua, C. Flow injection determination of p-aminophenol at trace level using inhibited luminol–dimethylsulfoxide–NaOH–EDTA chemiluminescence. *Water Res.* **2005**, *39*, 396–402.
3. Harmon, R.C.; Kiningham, K.K.; Valentovic, M.A. Pyruvate reduces 4-aminophenol in vitro toxicity. *Toxicol. Appl. Pharmacol.* **2006**, *213*, 179–186. [[CrossRef](#)] [[PubMed](#)]
4. Fedotov, A.V.; Grigoriev, V.S.; Svittsov, A.A. Organic Wastewater Treatment and Concentration by Sorption Combined with Microfiltration. *J. Water Chem. Technol.* **2018**, *40*, 302–306. [[CrossRef](#)]
5. Lim, M.; Patureau, D.; Heran, M.; Lesage, G.; Kim, J. Removal of organic micropollutants in anaerobic membrane bioreactors in wastewater treatment: Critical review. *Environ. Sci. Water Res. Technol.* **2020**, *6*, 1230–1243. [[CrossRef](#)]
6. Pandey, S.; Fosso-Kankeu, E.; Redelinghuys, J.; Kim, J.; Kang, M. Implication of biofilms in the sustainability of acid mine drainage and metal dispersion near coal tailings. *Sci. Total Environ.* **2021**, *788*, 147851. [[CrossRef](#)] [[PubMed](#)]
7. Frappa, M.; Macedonio, F.; Drioli, E. Progress of Membrane Engineering for Water Treatment. *J. Membr. Sci. Res.* **2020**, *6*, 269–279.
8. Aliyu, U.M.; Rathilal, S.; Isa, Y.M. Membrane desalination technologies in water treatment: A review. *Water Pract. Technol.* **2018**, *13*, 738–752. [[CrossRef](#)]
9. Pangarkar, B.; Deshmukh, S.; Sapkal, V. Review of membrane distillation process for water purification. *Desalin. Water Treat.* **2014**, *57*, 2959–2981. [[CrossRef](#)]
10. Wang, J.; Zhuan, R. Degradation of antibiotics by advanced oxidation processes: An overview. *Sci. Total Environ.* **2020**, *701*, 135023. [[CrossRef](#)]
11. Liu, H.; Wang, C.; Wang, G. Photocatalytic Advanced Oxidation Processes for Water Treatment: Recent Advances and Perspective. *Chem. Asian J.* **2020**, *15*, 3239–3253. [[CrossRef](#)]
12. Fosso-Kankeu, E.; Pandey, S.; Ray, S.S. *Photocatalysts in Advanced Oxidation Processes for Wastewater Treatment*; Fosso-Kankeu, E., Pandey, S., Ray, S.S., Eds.; John Wiley & Sons: Hoboken, NJ, USA, 2020; p. 320.
13. Yang, X.Y.; Chen, Y.; Liu, X.B.; Guo, F.C.; Su, X.X.; He, Q. Influence of titanium dioxide nanoparticles on functionalities of constructed wetlands for wastewater treatment. *Chem. Eng. J.* **2018**, *352*, 655–663. [[CrossRef](#)]
14. Rupa, E.J.; Kaliraj, L.; Abid, S.; Yang, D.-C.; Jung, S.-K. Synthesis of a Zinc Oxide Nanoflower Photocatalyst from Sea Buckthorn Fruit for Degradation of Industrial Dyes in Wastewater Treatment. *Nanomaterials* **2019**, *9*, 1692. [[CrossRef](#)]
15. García, A.; Delgado, L.; Torà, J.A.; Casals, E.; González, E.; Puentes, V.; Font, X.; Carrera, J.; Sánchez, A. Effect of cerium dioxide, titanium dioxide, silver, and gold nanoparticles on the activity of microbial communities intended in wastewater treatment. *J. Hazard. Mater.* **2012**, *199–200*, 64–72. [[CrossRef](#)]
16. Yahya, N.; Aziz, F.; Jamaludin, N.; Mutalib, M.A.; Ismail, A.; Salleh, W.W.; Jaafar, J.; Yusof, N.; Ludin, N.A. A review of integrated photocatalyst adsorbents for wastewater treatment. *J. Environ. Chem. Eng.* **2018**, *6*, 7411–7425. [[CrossRef](#)]
17. Montalvo, S.; Huiliñir, C.; Borja, R.; Sánchez, E.; Herrmann, C. Application of zeolites for biological treatment processes of solid wastes and wastewaters—A review. *Bioresour. Technol.* **2020**, *301*, 122808. [[CrossRef](#)]
18. Zhu, Q.; Moggridge, G.D.; D’Agostino, C. Adsorption of pyridine from aqueous solutions by polymeric adsorbents MN 200 and MN 500. Part 2: Kinetics and diffusion analysis. *Chem. Eng. J.* **2016**, *306*, 1223–1233. [[CrossRef](#)]
19. Adnan, S.; Hoang, M.; Wang, H.T.; Xie, Z.L. Commercial PTFE membranes for membrane distillation application: Effect of microstructure and support material. *Desalination* **2012**, *284*, 297–308. [[CrossRef](#)]
20. Astakhov, E.Y.; Shutov, A.A. Porous polytetrafluoroethylene film. *Tech. Phys. Lett.* **2007**, *33*, 228–230. [[CrossRef](#)]
21. Feng, S.; Zhong, Z.; Wang, Y.; Xing, W.; Drioli, E. Progress and perspectives in PTFE membrane: Preparation, modification, and applications. *J. Membr. Sci.* **2018**, *549*, 332–349. [[CrossRef](#)]
22. Yang, Y.; Strobel, M.; Kirk, S.; Kushner, M.J. Fluorine Plasma Treatments of Poly(propylene) Films, 2—Modeling Reaction Mechanisms and Scaling. *Plasma Process. Polym.* **2010**, *7*, 123–150. [[CrossRef](#)]
23. Calcagno, L.; Compagnini, G.; Foti, G. Structural modification of polymer films by ion irradiation. *Nuclear Instrum. Methods Phys. Res.* **1992**, *65*, 413–422. [[CrossRef](#)]
24. Ding, Z.-Y.; Aki, S.N.V.K.; Abraham, M.A. Catalytic Supercritical Water Oxidation: Phenol Conversion and Product Selectivity. *Environ. Sci. Technol.* **1995**, *29*, 2748–2753. [[CrossRef](#)] [[PubMed](#)]
25. Yu, J.; Savage, P.E. Catalytic Oxidation of Phenol over MnO₂ in Supercritical Water. *Ind. Eng. Chem. Res.* **1999**, *38*, 3793–3801. [[CrossRef](#)]
26. Oshima, Y.; Tomita, K.; Koda, S. Kinetics of the Catalytic Oxidation of Phenol over Manganese Oxide in Super-critical Water. *Ind. Eng. Chem. Res.* **1999**, *38*, 4183–4188. [[CrossRef](#)]
27. Sakarkar, S.; Muthukumar, S.; Jegatheesan, V. Polyvinylidene Fluoride and Titanium Dioxide Ultrafiltration Photocatalytic Membrane: Fabrication, Morphology, and Its Application in Textile Wastewater Treatment. *J. Environ. Eng.* **2020**, *146*, 04020053. [[CrossRef](#)]
28. al Aani, S.; Mustafa, T.N.; Hilal, N. Ultrafiltration membranes for wastewater and water process engineering: A comprehensive statistical review over the past decade. *J. Water Process Eng.* **2020**, *35*, 101241. [[CrossRef](#)]
29. Wang, W.; Wang, Y.; Wang, L. Study on the Mechanism of Removal of Formaldehyde by MnO₂. *Non-Ferr. Min. Metall.* **2008**, *24*, 49–51.

30. Liu, Y.; Luo, M.; Wei, Z.; Xin, Q.; Ying, P.; Li, C. Catalytic oxidation of chlorobenzene on supported manganese oxide catalysts. *Appl. Catal. B Environ.* **2001**, *29*, 61–67. [[CrossRef](#)]
31. Betterton, E.A.; Hoffmann, M.R. Kinetics and mechanism of the oxidation of aqueous hydrogen sulfide by peroxymonosulfate. *Environ. Sci. Technol.* **1990**, *24*, 1819–1824. [[CrossRef](#)]
32. Wang, Y.; Sun, P.H.; Ang, H.M.; Tade, M.; Wang, S. Facile Synthesis of Hierarchically Structured Magnetic MnO₂/ZnFe₂O₄ Hybrid Materials and Their Performance in Heterogeneous Activation of Peroxymonosulfate. *ACS Appl. Mater. Interfaces* **2014**, *6*, 19914–19923. [[CrossRef](#)] [[PubMed](#)]
33. Yao, Y.; Xu, C.; Yu, S.; Zhang, D.; Wang, S. Facile Synthesis of Mn₃O₄—Reduced Graphene Oxide Hybrids for Catalytic Decomposition of Aqueous Organics. *Ind. Eng. Chem. Res.* **2013**, *52*, 3637–3645. [[CrossRef](#)]
34. Stobbe, E.R.; De Boer, B.A.; Geus, J.W. The reduction and oxidation behaviour of manganese oxides. *Catal. Today* **1999**, *47*, 161–167. [[CrossRef](#)]
35. Gandhe, A.R.; Rebello, J.S.; Figueiredo, J.; Fernandes, J. Manganese oxide OMS-2 as an effective catalyst for total oxidation of ethyl acetate. *Appl. Catal. B Environ.* **2007**, *72*, 129–135. [[CrossRef](#)]
36. Saputra, E.; Muhammad, S.; Sun, P.H.; Ang, H.-M.; Tade, M.; Wang, S. A comparative study of spinel structured Mn₃O₄, Co₃O₄ and Fe₃O₄ nanoparticles in catalytic oxidation of phenolic contaminants in aqueous solutions. *J. Colloid Interface Sci.* **2013**, *407*, 467–473. [[CrossRef](#)]